Carbohydrate Polymers 289 (2022) 119385

Contents lists available at ScienceDirect

Carbohydrate Polymers

journal homepage: www.elsevier.com/locate/carbpol

Enhancing the antibacterial effect of chitosan to combat orthopaedic implant-associated infections

Dien Puji Rahayu [1], Arianna De Mori, Rahmi Yusuf, Roger Draheim, Aikaterini Lalatsa, Marta Roldo [*]

School of Pharmacy and Biomedical Sciences, University of Portsmouth, St Michael's Building, White Swan Road, Portsmouth PO1 2DT, United Kingdom

ARTICLE INFO

Keywords:
Chitosan
Chitosan derivatives
Antibacterial activity
S. aureus
Implant-associated infection

ABSTRACT

The development of antibacterial resistance imposes the development of novel materials to relieve the burden of infection. Chitosan, a material of natural and sustainable origin, possesses ideal characteristics to translate into a novel biomaterial with antibacterial properties, as it already has these properties and it allows easy and scalable chemical modification to enhance its activity. The aim of the present work was that of producing low molecular weight chitosans that have higher solubility and can remain protonated at physiological pH, thus enhancing the antimicrobial action. This was achieved by reacting acid hydrolysed low molecular weight chitosan with 2-bromoethyleneamine hydrobromide or Fmoc-Lys(Fmoc)-OH to elicit *N*-(2-ethylamino)-chitosan and *N*-2(2,6-diaminohexanamide)-chitosan polymers. The latter derivative, CS3H Lys, that was synthesised for the first time, showed superior efficacy against *Staphylococcus aureus*, supporting further studies for its inclusion in implant coating materials to tackle the burden of orthopaedic implant-associated infections.

1. Introduction

Novel antimicrobial materials to limit usage of current antibiotics, against which many bacteria have developed resistance, are increasingly needed for surgical interventions (Mullis et al., 2021). Of particular interest is the development of coating materials for implantable devices prone to infection mainly by *Staphylococcus aureus* (Oliveira et al., 2018). Infection remains the main reason for failure of orthopaedic implants with serious implications for individual patients who often require a second surgery, removal of the implant and a long-stay in hospital. Thus, these infections are not only debilitating for the patient but also costly for national health services (Arciola & Campoccia, 2018). Chitin and chitosan biomaterials are sustainable and recyclable waste materials that possess natural antibacterial properties, which can be enhanced by chemical modification, and are widely studied as coatings for implantable devices (Roldo & Fatouros, 2011). Chitosan is effective against a wide range of target organisms and available in a variety of formulations (solutions, films, composites) (Abd El-Hack et al., 2020; Costa-Pinto et al., 2021). Molecular weight (MW), degree of deacetylation (DD) and chemical modification of chitosan determine the physicochemical properties and biological activities of the polymer, including its antibacterial effects. Formulation parameters are also critical to their successful application and these include the concentration, pH, physical form and ionic strength (Costa-Pinto et al., 2021; Yuan et al., 2011). The antibacterial activity of chitosan and its derivatives has been studied from the early 1980s, while different mechanisms and combination of mechanisms have been suggested, researchers more generally agree on its complexity and its dependence on factors such as molecular weight, degree of deacetylation and physical form (Goy et al., 2009; Tan et al., 2013). One of the suggested mechanisms of action is based on the electrostatic interaction between chitosan positively charged amino groups and the predominantly anionic lipopolysaccharide (LPS) on Gram-negative bacteria or teichoic acid on Gram-positive bacteria (Kulawik et al., 2019). In Gram-negative bacteria, chitosan interacts with LPS molecules and displaces divalent cations (e.g., Ca^{2+} and Mg^{2+}) inducing depolarisation of the cell membrane, resulting in increased permeability, osmotic damage, intercellular leakage and ultimately cell death. In Gram-positive bacteria, chitosan diffuses inside the cell, binds to the cellular membrane, and inhibits their growth (Chao et al., 2019). Studies on ultra high molecular weight chitosan suggest also a mechanism of engulfment by chitosan, whereby chitosan coated cells slowly rupture and decompose (Li et al., 2016). And more recent

* Corresponding author.
E-mail address: marta.roldo@port.ac.uk (M. Roldo).
[1] Present address: National Research and Innovation Agency of Indonesia (BRIN), Lebak Bulus Raya No. 49 Jakarta 12440, Indonesia.

https://doi.org/10.1016/j.carbpol.2022.119385
Received 6 October 2021; Received in revised form 17 March 2022; Accepted 18 March 2022
Available online 28 March 2022

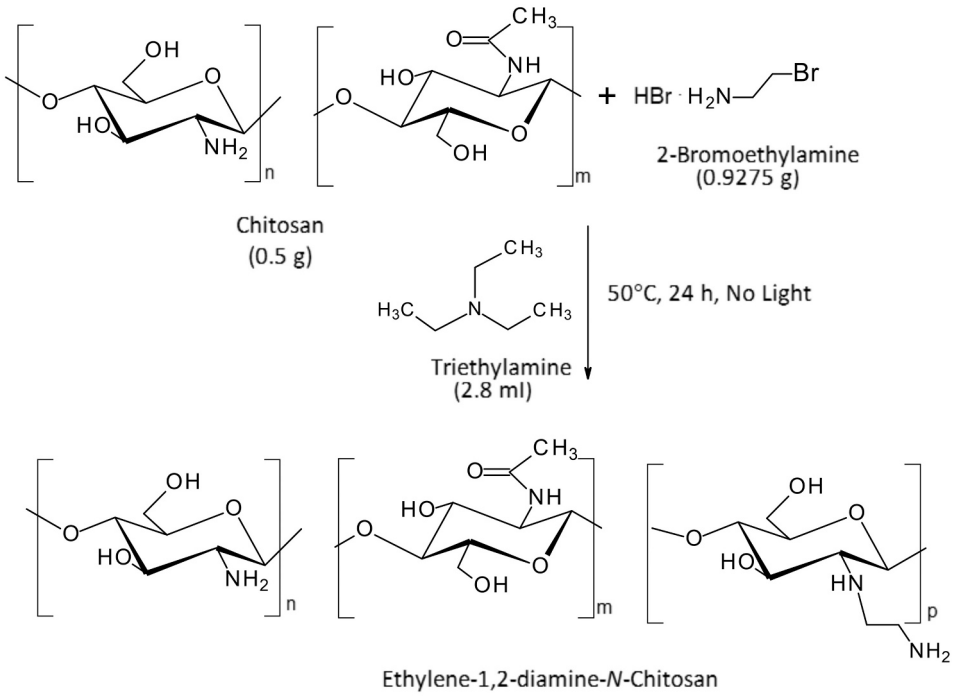

Scheme 1. Synthesis of *N*-(2-ethylamino)-chitosan.

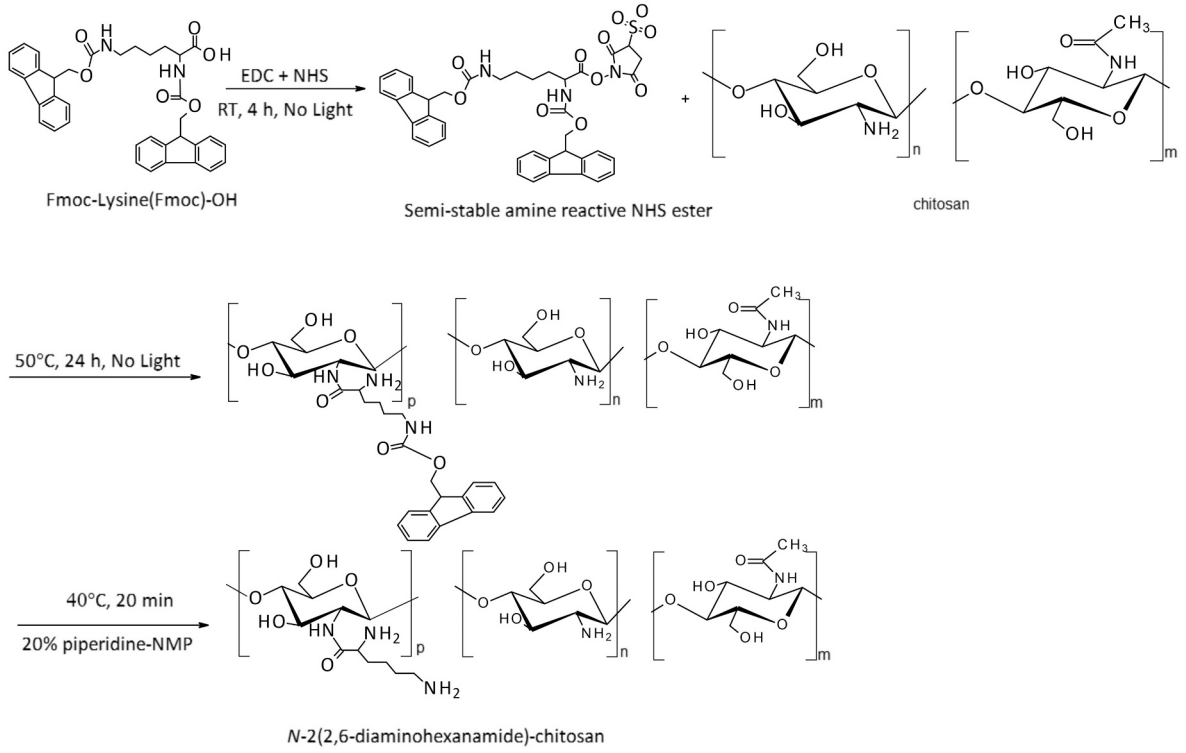

Scheme 2. Synthesis of *N*-2(2,6-diaminohexanamide)-chitosan.

studies, looking at chitosan fibers, highlight the complex relation between molecular weight and degree of deacetylation in determining the antibacterial effect (Li et al., 2022). Various chitosan derivatives have been engineered to maintain the cationic charge or enhance it by introducing more reactive amino groups onto the chitosan backbone. Rahmani et al. successfully synthesised 4-*N*, *N* dimethyl amino benzyl *N*, *O* carboxymethyl chitosan achieving a higher positive charge at pH 7.2, higher solubility and more effective antibacterial activity against *Escherichia coli*, *S. aureus* and *Staphylococcus epidermidis* (Rahmani et al., 2016). By introducing the quaternary amine group using glycidyl trimethyl ammonium chloride, Cheah et al. formed a quaternized chitosan nanofiber membrane, and reported that the antibacterial activity against *E. coli* was enhanced by two-fold compared to unmodified chitosan (Cheah et al., 2019). Hu et al. synthesised and tested the antibacterial

Table 1
Reaction yields (mean ± SD, $n = 3$) and molecular weight of chitosan polymers as determined by GPC/LALLS.

Polymer	Reaction yield (%)	Mw (g mol^{-1})	Mn	Mw/Mn
CS	N/A	1.653×10^5	4.229×10^4	3.909
CS3H	89.5 ± 1.8	4.709×10^4	4.156×10^4	1.133
CS3H EtNH$_2$	75.1 ± 2.8	- Could not be measured -		
CS3H Lys	74.4 ± 3.5	3.345×10^4	1.893×10^4	1.768

activity of 6-amino-ethylamino-6-deoxy chitosan, 6-butyl-amino-6-deoxy chitosan, and 6-pyridyl-6-deoxy chitosan. These modified chitosan derivatives showed higher antibacterial activity compared to streptomycin against *S. aureus*, *E. coli*, *Bacillus anthracis*, *Bacillus subtilis*, and *Salmonella enterica* serovar Thypi (Hu et al., 2016).

Several reports support that a higher degree of deacetylation (DD) enhances the antibacterial properties of chitosan by increasing the charge density along the polymer (Goy et al., 2009; Rahmani et al., 2016), although more investigation is needed to identify whether the enhanced activity is specifically linked to the DD value or more generally to an increase in water solubility. Less consensus has been achieved on the effect of molecular weight (MW). In a comparative study, low MW (107 kDa) chitosans showed higher antibacterial activity against *Aggregatibacter actinomycetemcomitans* and *Prevotella buccae*, while high MW (624 kDa) chitosan was more effective against *Streptococcus mutans* and *Tannerella forsythensis* (Costa et al., 2012). Against *S. aureus*, chitosans of 50–225 kDa were more effective than those of 10–35 kDa, with a further reduction in activity observed for chitosan oligomers (2–4 kDa) (Sahariah et al., 2019). Similarly high (600–800 kDa) MW chitosans were more effective than chitosan with low MW (100 kDa) against the

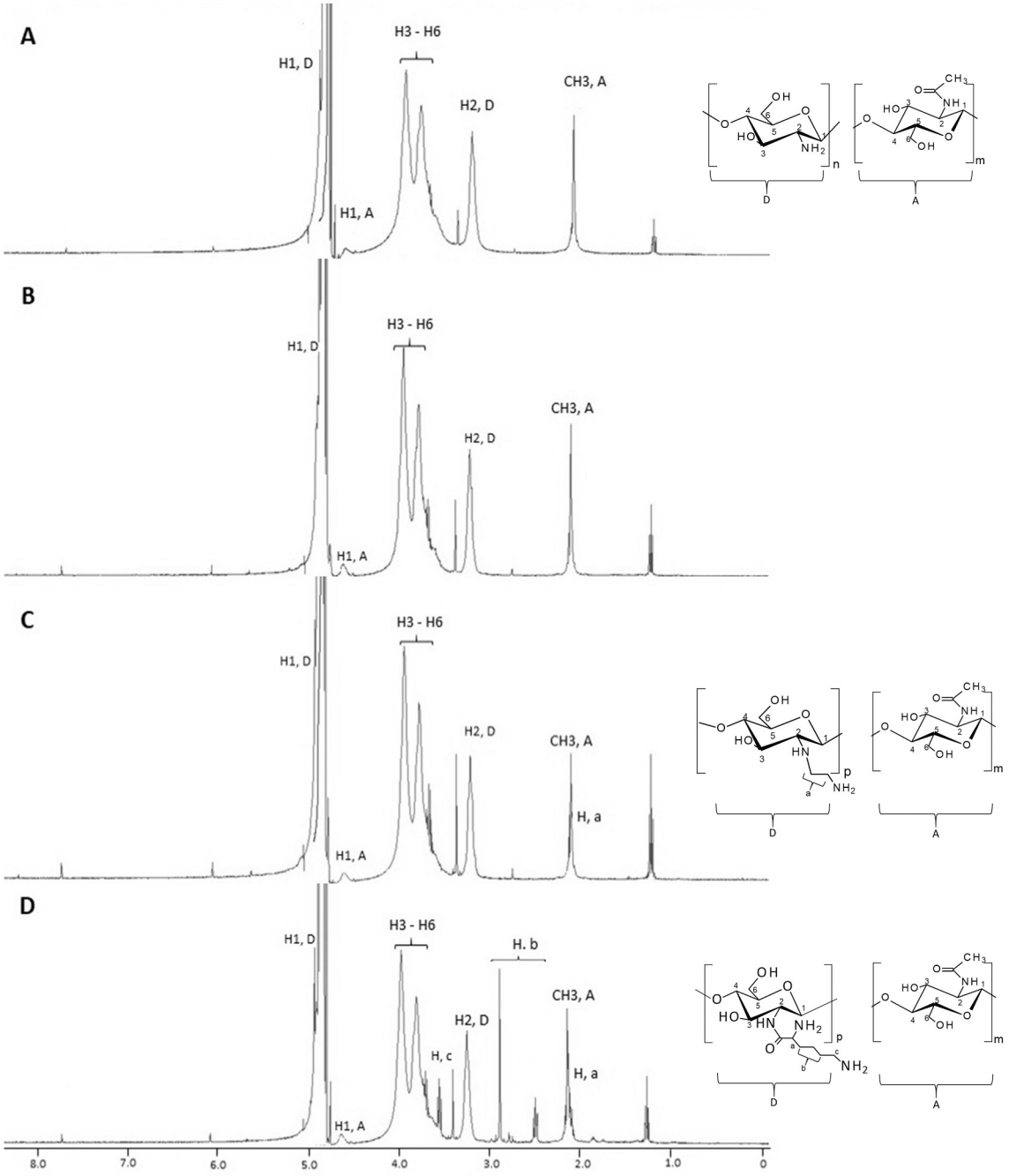

Fig. 1. ^{1}H NMR spectra of chitosan polymers. (A) CS, (B) CS3H, (C) CS3H EtNH$_2$, and (D) CS3H Lys.

Table 2
Results of elemental analysis and calculated C/N ratio and degree of substitution (DS) values; degree of acetylation (DA) as calculated from ^{1}H NMR (mean ± SD, $n = 3$); and pKa values calculated by titration (mean ± SD, n = 3). One-way ANOVA for DA $p > 0.05$ and pKa $p < 0.05$, Dunnett's multiple comparisons: *p < 0.05; **$p < 0.01$; ***$p < 0.001$.

Sample	Elemental composition					DA (%)	pKa value ± SD
	C (%)	H (%)	N (%)	C/N	DS		
CS	40.59 ± 0.05	7.96 ± 0.04	7.33 ± 0.06	5.53	N/A	15.37 ± 0.47	6.38 ± 0.01
CS3H	33.27 ± 0.04	7.15 ± 0.06	6.06 ± 0.04	5.49	N/A	14.20 ± 0.17	6.68 ± 0.06***
CS3H $EtNH_2$	40.31 ± 0.08	7.26 ± 0.05	7.28 ± 0.16	5.54	0.03	14.03 ± 0.10	6.60 ± 0.04**
CS3H Lys	50.16 ± 0.05	7.22 ± 0.04	7.60 ± 0.03	6.60	0.18	17.56 ± 5.23	6.56 ± 0.06**

cariogenic microorganisms *S. mutans* and *Streptococcus sobrinus* (Abedian et al., 2019). It has been postulated that MW cannot be considered separate from other factors such as pH, DD, viscosity and bacteria examined. Here, we hypothesise that producing low MW (<50 kDa) chitosans that possess higher solubility and remain protonated at physiological pH will elicit greater antibacterial activity. To attain these characteristics, low MW chitosan polymers were modified by adding ethylamine or lysine moieties. These grafted polymers enable the protonated amine to be less sterically hindered and remain protonated at physiological pH enhancing the overall aqueous solubility and cationic charge at physiological pH of the polymers. Even though numerous chitosan derivatives have been prepared, to the best of our knowledge, there are no reports of the synthesis and characterisation of *N*-(2-ethylamino)-chitosan and *N*-2(2,6-diaminohexanamide)-chitosan. These novel low MW polymers were tested for their antimicrobial properties against *S. aureus* and *P. aeruginosa* and cytocompatibility with osteoblasts.

2. Materials and methods

2.1. Materials

Commercially available low-viscosity chitosan from shrimp shell (CAS 9012-96-4, Lot #BCBQ 3414V, MW: 165.3 kDa (GPC-LALLS), and DD 84.63%) was purchased from Sigma-Aldrich Inc. (Gillingham, Dorset, UK). All other chemicals used in this study were analytical grade and purchased from Sigma Aldrich Inc. (Gillingham, Dorset, UK), unless otherwise stated.

2.2. Preparation of low molecular weight chitosan hydrochloride (CS3H)

Chitosan (CS) was degraded in hydrochloric acid as previously described (Lalatsa et al., 2012). Briefly, chitosan (1 g) was dissolved in HCl (4 M, 72 ml) and heated to 50 °C under vigorous stirring. After 3 h, the reaction was stopped by cooling down the reaction mixture in an ice bath. The product was then dialysed (molecular weight cut off 12–14 kDa, Medicell Membranes Ltd. London, UK) against 5 l of distilled water with six changes over 24 h. The dialysed solution was freeze-dried and obtained as a white cotton-like material (CS3H).

2.3. Synthesis of N-(2-ethylamino)-chitosan (CS3H $EtNH_2$)

The synthesis of *N*-(2-ethylamino)-chitosan (CS3H $EtNH_2$) was adapted from the method developed by Gerecht et al. for the derivatization of dextran (Scheme 1) (Gerecht et al., 2011). CS3H (0.5 g) was dispersed in *N*-methyl-2-pyrrolidone (NMP, 50 ml, Rathburn Chemicals Ltd. Scotland, UK) in the presence of triethylamine (2.8 ml). To this, a solution of 2-bromoethyleneamine hydrobromide (BEAHB, 0.9375 g) in NMP (3 ml) was added dropwise. The reaction was stirred at 50 °C and protected from light. After 24 h, the product was precipitated by addition of ice cold ether (30 ml) and centrifuged (2000 rpm, 10 min). The product was collected and dialysed (MWCO: 12–14 kDa) against 500 ml cold ethanol for 1 h (twice) followed by dialysis against 5 l of distilled water with six changes over 24 h. The dialysate was lyophilised, and a white cotton-like product was obtained.

2.4. Synthesis of N-2(2,6-diaminohexanamide)-chitosan (CS3H Lys)

The method for the synthesis of *N*-2(2,6-diaminohexanamide)-chitosan was adapted from the procedure developed by Romanelli et al. for the production of Fmoc-protected-valine derivatives of peptides (Scheme 2) (Romanelli et al., 2015). CS3H was reacted with Fmoc-Lys (Fmoc)-OH (N_α,N_ε-di-Fmoc-L-lysine, CAS #78081-87-5) in the presence of 1-ethyl-3-(3-dimethylamino) propyl carbodiimide (EDC) and *N*-hydroxysuccinimide (NHS). Briefly, to a solution of Fmoc-protected

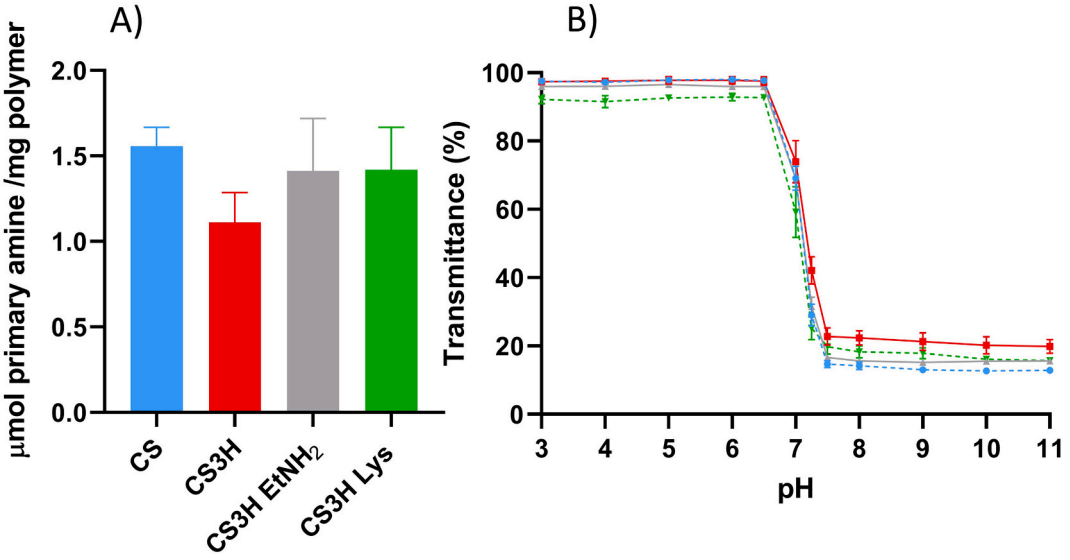

Fig. 2. A) Determination of amino groups on chitosan and its derivatives by TNBS assay. Data are reported as mean ± SD ($n = 3$); one-way ANOVA ($p > 0.05$). B) UV transmittance at 600 nm of polymeric solutions as a function of pH. CS; CS3H; CS3H $EtNH_2$; CS3H Lys. Data are reported as mean ± SD (n = 3).

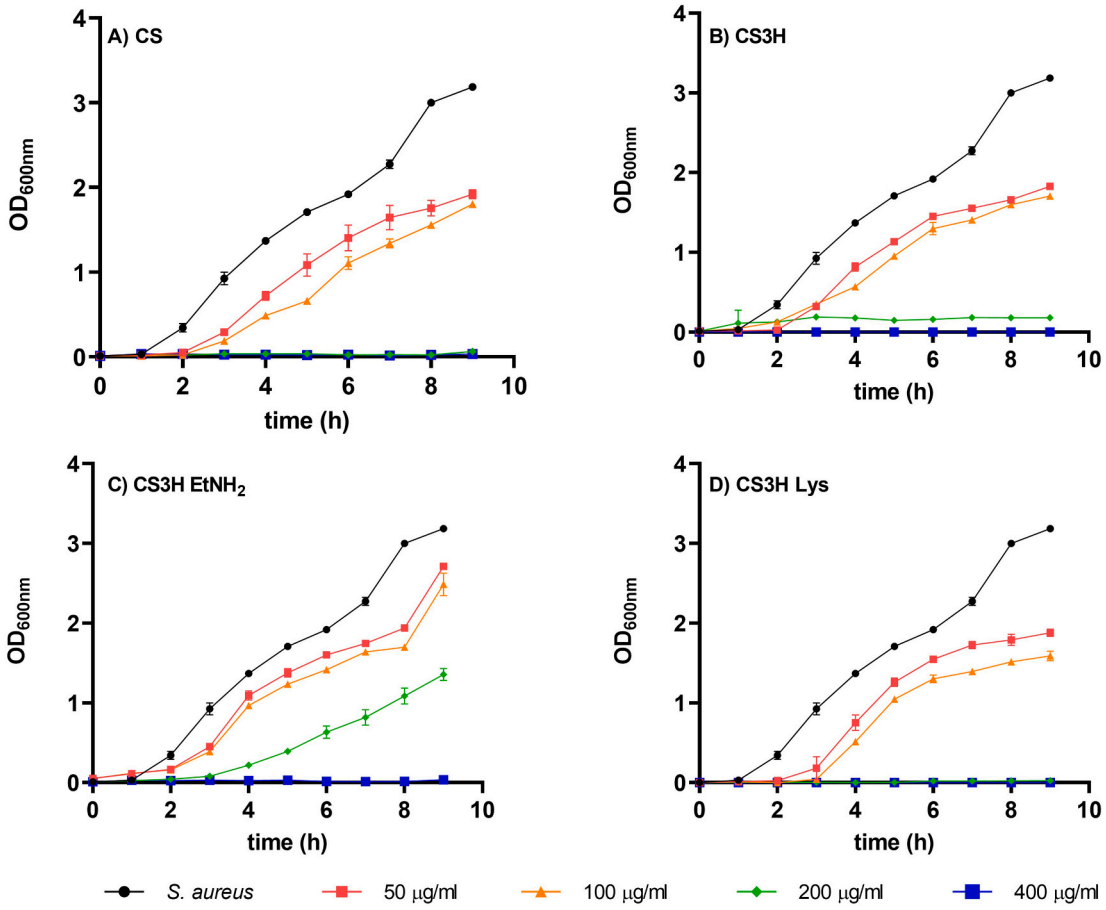

Fig. 3. Growth curves of *S. aureus* in LB medium at 37 °C in the presence of different concentrations of chitosan polymers. Results are reported as a mean ± SD (n = 3). Two-way ANOVA for all polymers found a statistically-significant effect on average bacterial growth dependent on both concentration ($p < 0.0001$) and time ($p < 0.0001$) with statistically significant interactions ($p < 0.0001$). Post-hoc Bonferroni test found statistically significant difference between all concentrations tested ($p < 0.0001$) apart from between 200 and 400 μg/ml for CS3H Lys ($p > 0.05$).

lysine (1.54 g, 2.6 mmol, 1 Equiv) in *N*-methyl-2-pyrrolidone (NMP, 20 ml), stirred at room temperature for 1 h to allow complete dissolution, the following were added: EDC (0.85 g, 4.42 mmol, 1.7 Equiv) in 4 ml of NMP, and NHS (0.15 g, 1.3 mmol, 0.5 Equiv) in 1 ml of NMP. The reaction was left to proceed under stirring at room temperature for 3 h and was protected from light. CS3H (1% w/v, 0.5 g) in NMP (50 ml) was added and the pH was adjusted to >7.5 using NaOH (1 M in NMP). The reaction mixture was stirred at 40 °C for further 24 h. Fmoc was then removed by adding piperidine (20% v/v, 6 ml) and stirring at 40 °C for 20 min. The product was filtered with Whatman No. 1 filter paper, and the deprotection process was repeated four times for the filtrate. The product was collected and dialysed (MWCO: 12–14 kDa) against 5 l of distilled water with 6 changes over 24 h. The dialysate was lyophilised, and a white product was obtained.

2.5. Characterisation of the modified chitosan polymers

2.5.1. Molecular weight determination (GPC-LALLS)

Weight-average molecular weight (MW), number-average molecular weight (Mn) and molecular weight distribution (MW/Mn) were measured using gel permeation chromatography and low angle light scattering (GPC-LALLS) (Wyatt Technology, Santa Barbara, CA). A low-angle laser light scattering (LALLS) detector with three detection angles (2, 90 and 135°), laser wavelength λ = 658 nm (mini Dawn Treos, Wyatt Technology, Santa Barbara, CA), and an interferometric refractometer (Optilab, Wyatt Technology, Santa Barbara, CA) were connected to the GPC system. The mobile phase was acetate buffer (0.3 M anhydrous sodium acetate, 0.2 M glacial acetic acid, pH = 4.5) (Lalatsa et al., 2012). Samples were filtered (0.2 μm polyethersulfone (PES) filter, Millipore Millex-HA) and injected using a rheodyne injector equipped with 100 μl injection loop. Measurements were performed at room temperature with a mobile phase flow rate of 0.5 ml min^{-1} (Jasco PU-980 isocratic pump, Tokyo, Japan). The data were analysed using ASTRA for windows version 6 software (Wyatt Technology Corporation). Bovine serum albumin was used a standard to check column separation performance (Lalatsa et al., 2015; Siew et al., 2012).

2.5.2. ^1H NMR spectroscopy

^1H NMR spectra were recorded using a 400 MHz Nuclear Magnetic Resonance Spectrometer (JEOL, Oxford Instruments, Abingdon, UK), and analysed with JEOL Delta (v5.0.1) software. CS (15 mg) was dissolved in a few drops of deuterium chloride 20% w/v and diluted with 1 ml of deuterium oxide (DLM-4-100, Cambridge Isotope Lab, Leicestershire, UK) containing 0.04% of 3-(trimethylsilyl)-1-propanesulfonic acid sodium salt (DSS, CAS #2039-96-5). CS3H and CS3H Lys were dissolved 1 ml of D_2O. Integrals of characteristic signals were used to calculate the degree of deacetylation using Eq. (1) (Hirai et al., 1991):

$$DD(\%) = \left[1 - \frac{\frac{\int CH_3}{3}}{\frac{\int (H_2 - H_6)}{6}}\right] \times 100 \quad (1)$$

where $\int CH_3$ is the integral of the $-CH_3$ signal (~2 ppm) and $\int H_2\text{-}H_6$ is the sum of integrals of H_2 (~3.0–3.3 ppm), H_3, H_4, H_5, H_6, and H_6'

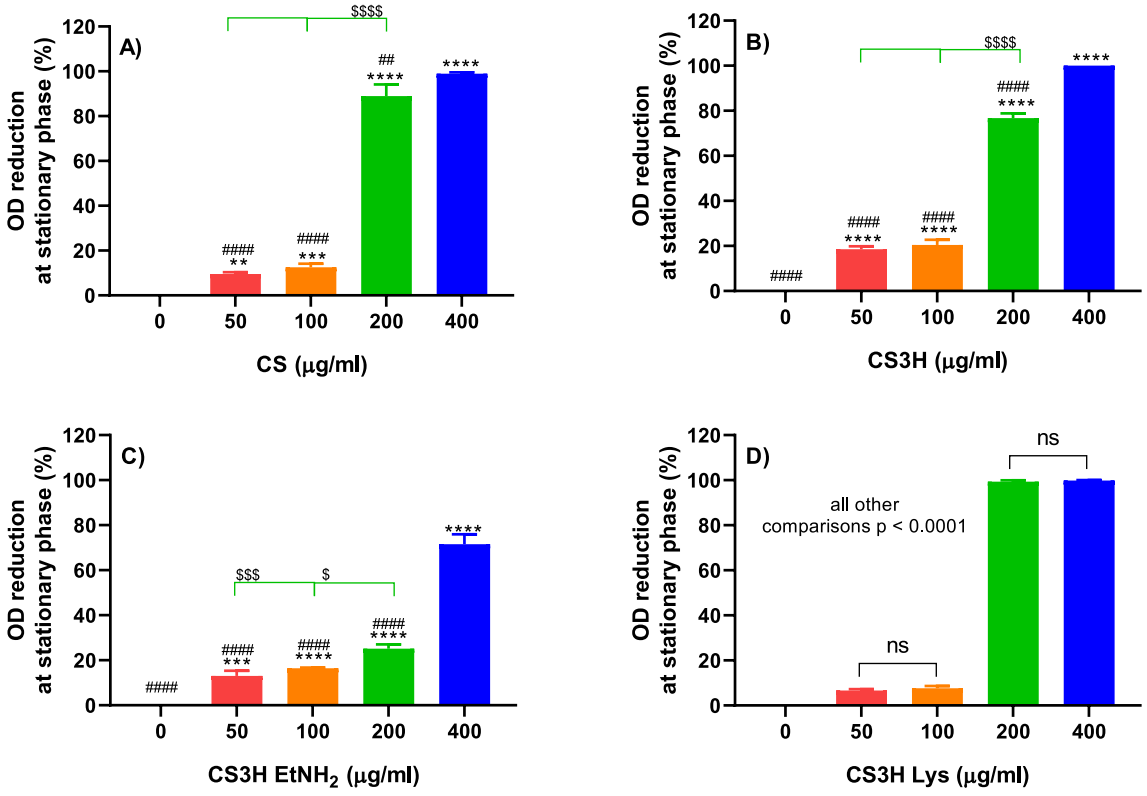

Fig. 4. Percentage reduction in OD_{600nm} at stationary phase for *S. aureus* grown in LB medium at 37 °C in the presence of chitosan polymers at different concentrations. Data are reported as mean ± SD ($n = 3$). Statistical significance of data was tested by one-way ANOVA and subsequently by Tukey's multiple comparison test. ($^{**}p < 0.01$, $^{***}p < 0.001$, $^{****}p < 0.0001$ compared to 0 μg/ml; $^{\#\#}p < 0.01$, $^{\#\#\#\#}p < 0.0001$ compared to 400 μg/ml and $^{\$}p < 0.05$, $^{\$\$\$}p < 0.001$, $^{\$\$\$\$}p < 0.0001$ for comparisons shown on graphs).

protons (~3.4–4.3 ppm).

2.5.3. Elemental analysis

The carbon, hydrogen and nitrogen (CHN) content was determined by elemental analysis using a Carlo-Erba (Thermo Flash 2000, Thermo Scientific, UK) elemental analyser. The degree of substitution (DS) was calculated applying Eq. (2) (Jiang et al., 2010):

$$DS = \frac{(C/N)_m - (C/N)_u}{n} \quad (2)$$

where $(C/N)_m$ is the C/N ratio of the chitosan derivative, $(C/N)_u$ is that of CS3H, n is the number of carbon atoms introduced after modification.

2.5.4. Potentiometric titration

Chitosan (0.05 g) was dissolved in 5 ml of HCl (0.1 M) and 10 ml of deionised water and stirred until completely dissolved. The chitosan solution was titrated with a dilute alkali solution (NaOH, 0.1 M) in known increments. Both the volume of NaOH added and pH values of the solution were recorded (Sivashankari & Prabaharan, 2016). The potentiometric titrations were monitored with a pH meter FE20 (Mettler Toledo, Greifensee, Switzerland). A titration curve of pH versus NaOH volume was drawn, and the midpoint calculated (Figs. S1 and S2) to find the pKa value (Kasaai, 2009).

2.5.5. Amine quantification

The amine content was determined by a 2,4,6-trinitrobenzene sulfonic acid (TNBS, Fisher Scientific, Loughborough, UK) assay. A fresh 0.1 M $NaHCO_3$ buffer solution was prepared, and the final pH adjusted with NaOH (1 M) to 8.5. Each sample (20 mg) was swelled in 10 μl HCl (1 M); deionised water (990 μl) was then added before adjusting the total volume to 10 ml with 0.1 M $NaHCO_3$. TNBS (5% in methanol, 0.25 ml) was added to 0.5 ml of each sample, mixed and incubated at 37 °C in a shaking incubator for 2 h. Sodium dodecyl sulfate (SDS, 0.25 ml, 10%) and HCl (0.125 ml, 1 M) were added to each sample, according to manufacturer's instructions. A standard curve was constructed with arginine (2–20 μg/ml) in 0.1 M $NaHCO_3$. Samples absorbance was measured at 335 nm (Multiskan Go UV–Vis spectrophotometer, Thermo Fisher Scientific, Paisley, UK).

2.5.6. Solubility studies

The pH dependence of chitosan polymers solubility was evaluated at room temperature by turbidimetry (Kubota et al., 2000). Samples (50 mg) were dissolved in 10 ml of aqueous acetic acid (10% v/v) and stirred for 1 h. The transmittance of the solutions was recorded, on a Nicolet e-100 spectrophotometer (Thermo Fisher Nicolet Corp., UK) using a quartz cell with an optical path length of 1 cm at 600 nm, after each stepwise addition (200 μl) of NaOH (5 M) until pH 12 (FE20 pH meter, Mettler Toledo, Greifensee, Switzerland).

2.6. Bacterial growth inhibition

Staphylococcus aureus (ATCC® 25923) and *P. aeruginosa* (ATCC® 27853), stored in Luria Broth (LB) medium and sterile glycerol 30% (1:1) at −80 °C, were transferred into 5 ml of fresh sterile LB medium by a sterile tip and incubated at 37 °C in 5% CO_2 atmosphere overnight. Bacteria were grown in 50 ml of sterile LB in 250 ml sterile flasks. Each flask contained approximately 1×10^6 CFU/ml (equal to 0.001 at OD_{600nm}) thoroughly mixed. Polymers stock solutions (20,000 μg/ml) were prepared in 0.5 M acetic acid; serial dilutions were performed to obtain 50, 100, 200, or 400 μg/ml test solutions and the pH was adjusted to 6.7 with NaOH (1 M). Media inoculated with bacteria and sterile media served as controls. Samples were incubated at 37 °C and 200 rpm

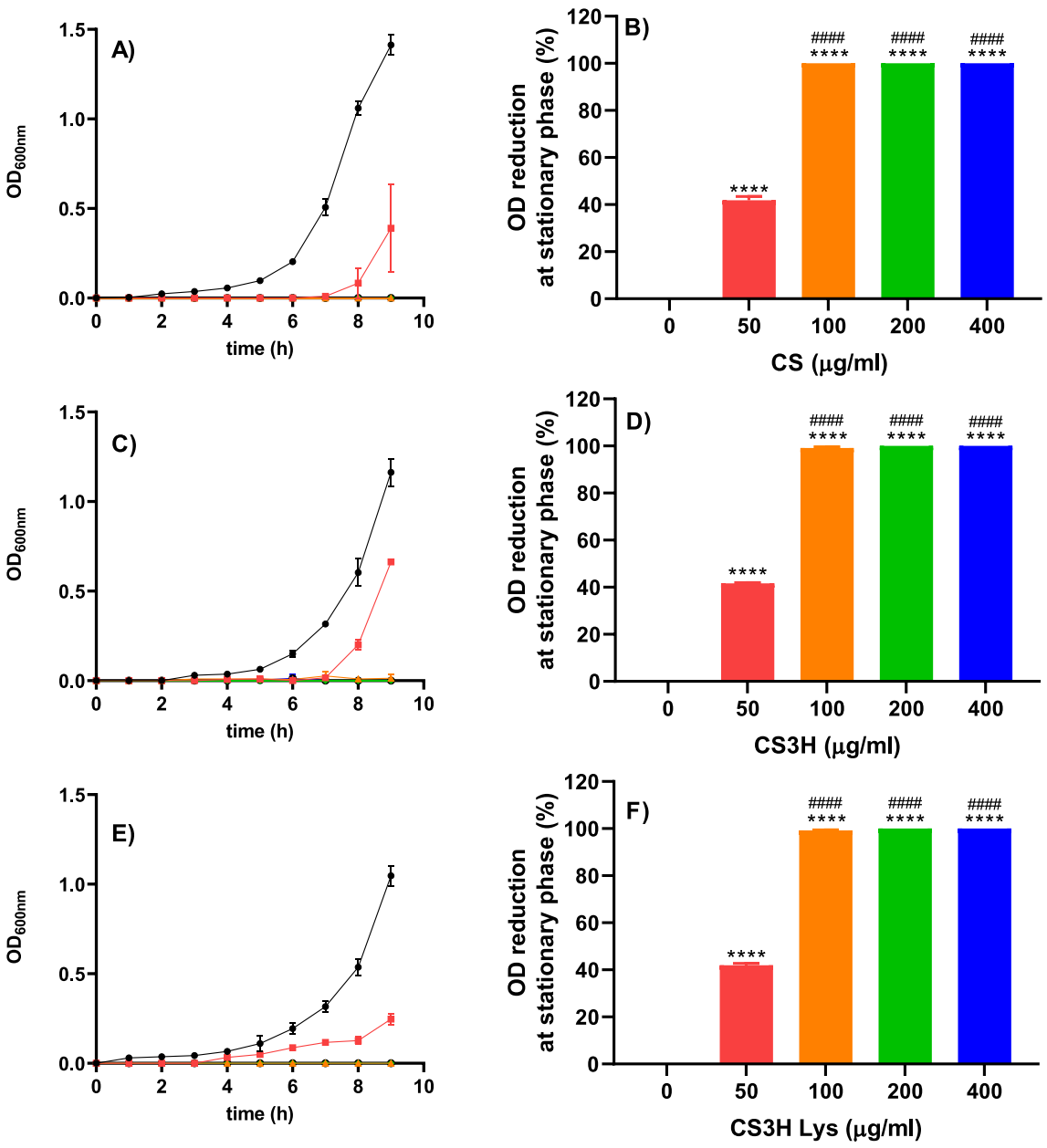

Fig. 5. Growth curves of *P. aeruginosa* in LB medium at 37 °C in the presence of different concentrations of A) CS, C) CS3H and E) CS3H Lys. Results are reported as a mean ± SD ($n = 3$). Two-way ANOVA for all polymers found a statistically-significant effect on average bacterial growth dependent on both concentration ($p < 0.0001$) and time ($p < 0.0001$) with statistically significant interactions ($p < 0.0001$). Post-hoc Bonferroni test found statistically significant difference between all concentrations tested compared to 0 and 50 μg/ml ($p < 0.0001$). Percentage reduction in OD_{600nm} at stationary phase for *P. aeruginosa* grown in LB medium at 37 °C in the presence of different concentrations of B) CS, D) CS3H and F) CS3H Lys. Data are reported as mean ± SD (n = 3). Statistical significance of data was tested by one-way ANOVA and subsequently by Tukey's multiple comparison test. (****$p < 0.0001$ compared to 0 μg/ml and $^{\#\#\#\#}p < 0.0001$ compared to 50 μg/ml).

(MaxQ™ 8000, Thermo Scientific, UK). Aliquots (1 ml) were removed from the culture every hour for 9 h (OD_{600nm}, cell density meter Ultrospec 10, Biosciences, Cambridge, UK). OD values were plotted as a function of time to obtain a growth curve. A single OD reading was taken at stationary phase, to calculate the overall percentage OD reduction.

2.7. Cytocompatibility studies

Human osteoblasts hFOB 1.19 (ATCC® CRL-11372™) were cultured in DMEM/F-12 containing 10% FBS, and 1% penicillin/streptomycin. Each polymer was prepared in acetic acid 0.5 M at the following concentrations 0, 50, 100, 200, 400, 800, and 1600 μg/ml, and the pH was adjusted to 6 with NaOH (0.1 M), this allowed the cell medium to maintain a neutral pH. Osteoblasts (passages 8–9) were plated in 96-well microtiter plates at a density 5×10^3 cells per well. Plates were incubated at 37 °C in an atmosphere of 5% of CO_2. After 24 h of incubation, cells were treated with the polymer solutions and incubated for 24 h. 3-[4,5-Dimetylthiazol]-2,2,5-diphenylterazolium bromide (MTT, 5 mg/ml) was dissolved in PBS, added to a final concentration of 0.5 mg/ml to each well and incubated for further 4 h. After removing the MTT/medium, the purple formazan crystals were dissolved in 100 μl of DMSO and absorbance was measured at 570 nm (SpectraMax i3x, Molecular Devices, Berkshire, UK).

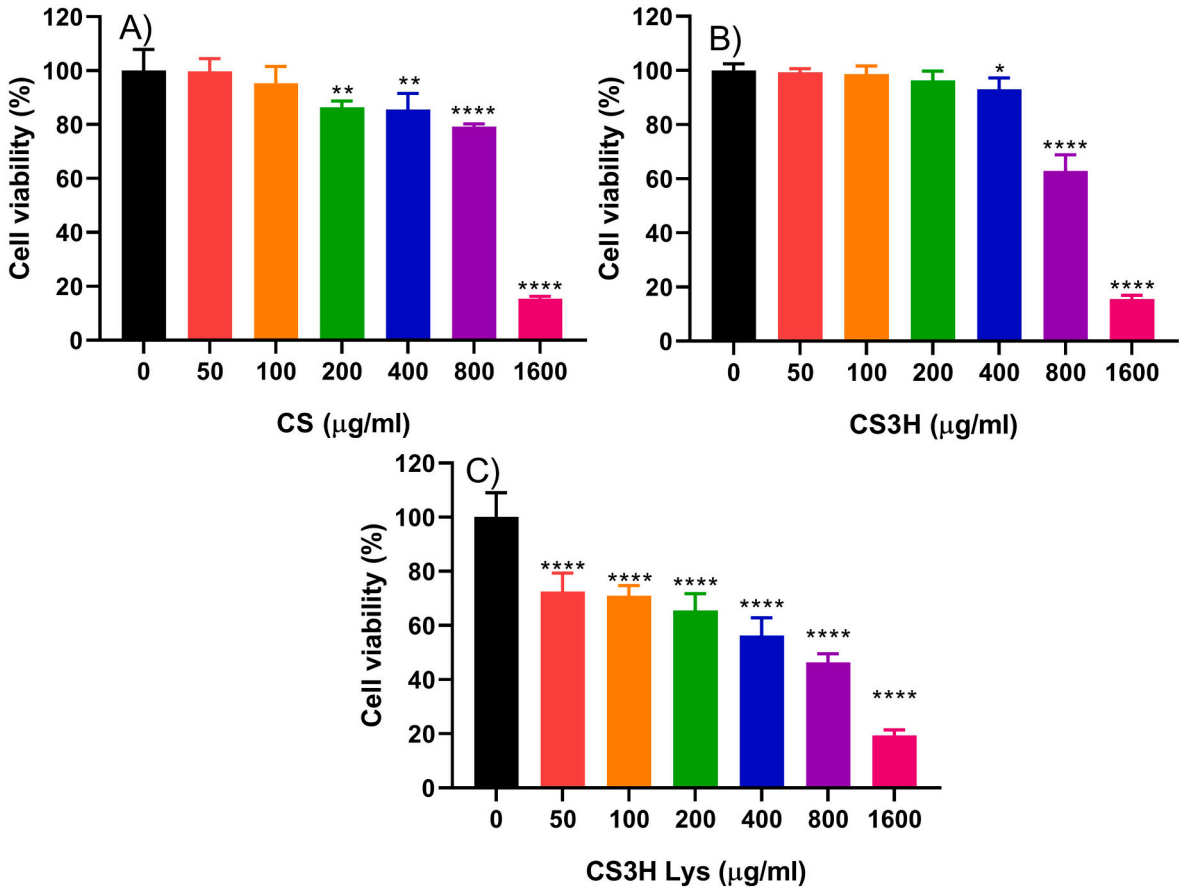

Fig. 6. Percentage viability of osteoblast cells grown in presence of different concentrations of A) CS; B) CS3H and C) CS3H Lys, as determined by MTT assay. Data are reported as mean ± SD ($n = 4$). Data were analysed by two-way ANOVA followed by Dunnett's multiple comparisons test (*$p < 0.05$; **$p < 0.01$; ****p < 0.0001).

2.8. Statistical analysis

All experiments were performed at least in triplicate and data are presented as mean ± standard deviation (SD). Data were analysed using GraphPad Prism version 8.2.1 for Windows, GraphPad Software, San Diego, California USA, www.graphpad.com. Details of the statistical analysis used are reported in figures and tables.

3. Results

3.1. Synthesis and characterisation of chitosan derivatives

Low molecular weight chitosan (CS3H, 47,090 Da) was obtained by acid hydrolysis of a chitosan polymer and used as starting polymer for the synthesis of CS3H $EtNH_2$ and CS3H Lys. All products were successfully obtained in a high (>70%) yield (Table 1).

The synthesis of modified chitosan (CS3H Lys) resulted in further reduction in molecular weight (33,450 Da). Since the molecular weight was derived by size exclusion chromatography combined with low angle light scattering (GPC-LALLS), absolute molecular weight was measured rather than relative molecular weight based on the retention time, which means that we can exclude aggregation or other conformational changes affecting the elution time and thus the calculated molecular weight. Both CS3H and CS3H Lys had lower polydispersity (PDI) compared to the original chitosan, as expected for low molecular weight degraded polymers (Lalatsa et al., 2012). All polymeric solutions were filtered through a 0.2 μm filter before injection into the GPC-LALLS; CS3H $EtNH_2$ was not completely soluble in the acetate buffer solution, which resulted in a loss of mass upon filtration that did not permit accurate analysis. Polymers were further characterised by ^{1}H NMR (Fig. 1). The ethylenamine peak of CS3H $EtNH_2$ was evident at 2.04 ppm (Fig. S3). The introduction of 2,6-diaminohexanoic in CS3H Lys was evidenced by new peaks at 2.038 ppm (overlapped with the acetyl group peak), 2.406–2.804 ppm, and at 3.481 ppm (Table S1, Figs. S3 and S4). The COSY spectrum for CS3H Lys (Fig. S5) further confirmed that the 2,6-diaminohexanoic chain was incorporated into the chitosan backbone based on the correlation peak between the proton from the acetyl group (2.049 ppm) with the proton from the CH in lysine (3.481 ppm). Modification was also evidenced by FTIR spectra (Fig. S6). ^{1}H NMR spectra were also used to determine the degree of acetylation (DA) which was not significantly affected by HCl hydrolysis ($p > 0.05$, Table 2). Also in the synthesis of CS3H $EtNH_2$ and CS3H Lys no significant change in the degree of acetylation compared to CS3H ($p > 0.05$ Dunnett's multicomparison test) was observed.

The C/N ratio, calculated by elemental analysis, of degraded chitosan decreased to 5.49 due to acid induced depolymerisation (Table 2), while the addition of carbon containing chains to CS3H NH_2 and CS3H Lys was confirmed by an increase in the C/N ratio to 5.54 and 6.60, respectively. The DS values of the chitosan derivatives were 0.03 and 0.18 for CS3H $EtNH_2$ and CS3H Lys, respectively. While there was no significant increase ($p > 0.05$) in the number of free amino groups, as detected by TNBS assay (Fig. 2A), the pKa of the degraded and modified chitosan was increased significantly ($p < 0.001$ and $p < 0.01$, respectively) thanks to the formation of the hydrochloride salt during dialysis (Fig. 2B). The other derivatives also showed higher pKa compared to the original chitosan. The increasing pKa means that the modified chitosan is soluble in a wider pH range (Fig. 2B). In acidic conditions (pH < 6.5), all polymers exhibited good water solubility (transmittance > 90%) due

to the protonation of the primary amine. However, when the pH was raised above 7, the transmittance of CS, CS3H, and CS3H Lys decreased (Mao et al., 2004; Panda et al., 2019). In general, the reduction of molecular weight, the addition of less hindered amino groups and the formation of hydrochloride salts all contributed to an increase in solubility of the polymers under study.

3.2. Inhibition of bacterial growth

The effect of chitosan and its derivatives on the growth curve of *S. aureus* was studied (Fig. 3).

At concentrations up to 100 μg/ml chitosan and its derivatives did not have a significant effect on the duration of the lag phase of *S. aureus*. At higher concentrations (200 μg/ml), the lag phase of CS, CS3H and CS3H Lys extended over 9 h, while CS3H $EtNH_2$ caused stress to the bacterial cells, resulting in a prolonged lag phase (up to 3 h) and a slower growth rate (Hamill et al., 2020). At the highest concentration (400 μg/ml), all chitosan polymers, except CS3H $EtNH_2$, showed complete growth inhibition (Fig. 4). CS3H Lys is the only polymer showing complete growth inhibition starting at 200 μg/ml demonstrating superior effect compared to chitosan and chitosan derivatives.

Due to the lower antibacterial effect of CS3H $EtNH_2$ this polymer was not further investigated, while the other polymers were tested also against the Gram-negative *P. aeruginosa* (Fig. 5). Although CS3H $EtNH_2$ could be more effective against other bacterial species, the limited solubility is likely to limit its applications, therefore this polymer was not studied further. *P. aeruginosa* was more susceptible to all treatments, with the 100 μg/ml dose causing complete growth inhibition by all polymers. CS3H Lys at 50 μg/ml had a slowing effect on the initial exponential growth phase of *P. aeruginosa* (Fig. 5E) but at stationary phase there was no statistical difference (one-way ANOVA $p > 0.05$) between the growth inhibition caused by the three polymers at this concentration.

3.3. Cytocompatibility study

The viability of osteoblast cells treated with various concentrations of chitosan polymers was tested (Fig. 6). CS and CS3H were relatively non-toxic to osteoblasts up to 400 μg/ml, while the CS3H Lys at the lowest concentration (50 μg/ml) elicited death of 30% of the cells. At 200 μg/ml CS3H Lys, a highly effective dose for preventing *S. aureus* growth, 66% of osteoblasts are viable.

4. Discussion

Molecular weight reduction of chitosans can be achieved by acid hydrolysis following a first order degradation (Lalatsa et al., 2012) in which both the glycosidic bonds (SN_1 reaction or depolymerisation) and the *N*-acetyl bonds (SN_2 reaction or deacetylation) are cleaved (Aljbour et al., 2019; Kasaai et al., 2013). The rate of SN_1 is similar to that of SN_2 in the presence of low concentration of acid, while in concentrated acid the rate of SN_1 becomes 10 times higher than the rate of SN_2 (Einbu & Vårum, 2007; Vårum et al., 1997). In the present work chitosan (165 kDa) was degraded by treatment with HCl 4 M at 50 °C, inducing the simultaneous activation of SN_1 and SN_2 processes. The acid hydrolysis successfully reduced the molecular weight and significantly decreased the degree of acetylation by around 1% ($p < 0.05$). The shorter polymer (CS3H) was successively modified by addition of 2-ethylanimo- (CS3H $EtNH_2$) and 2,6-diaminohexanoic- (CS3H Lys) moieties. Amino groups in the chitosan are attached directly to the polysaccharide backbone therefore being limited in their intermolecular interactions by steric hindrance. In order to reduce the steric hindrance, spacers of 2 and 6 carbon atoms were used. In the CS3H $EtNH_2$ synthesis, 2-bromoethylamine was reacted under alkaline conditions to obtain an intermediate cyclic ethylenimine derivative by the intramolecular attack of its primary amine that caused the halogen (Br) release (Hermanson, 2013). Fmoc-Lys(Fmoc)-OH was used in the CS3H Lys preparation in order to protect the amino groups in the amino acid chain, to avoid undesirable side reactions such as self-association of amino acid molecules. The chemical structure of chitosan and chitosan derivatives was confirmed by NMR, FTIR, and elemental analysis. NMR also confirmed the complete deprotection step of the Fmoc using piperidine (absence of Fmoc peaks at 7.2–7.8 ppm) (Zhang et al., 2009). The incorporation of 2-ethylanimo and 2,6-diaminohexanoic moieties did not increase the amine quantity significantly as corroborated by both the TNBS assay and elemental analysis. The cleavage of polymer chains using HCl and the addition of 2-ethylanimo and 2,6-diaminohexanoic groups succeeded in increasing the pKa, thus the solubility of the polymers at physiological pH. A clinical area in need of novel materials with antimicrobial properties is that of orthopaedic implants that are liable to infection caused in 66% of cases by Gram-positive *staphylococci*, more than half of which are *S. aureus* (Oliveira et al., 2018); of the minority infections (ca. 10%) caused by Gram-negative bacteria, 80% are caused by *P. aeruginosa* (Campoccia et al., 2006). Our results confirmed the ability of chitosan to inhibit the growth of *S. aureus*, as it is widely documented in literature (Abd El-Hack et al., 2020). Chitosan showed a dose-dependent effect, with changes to the growth curve observed at concentrations as low as 50 μg/ml and significant reduction ($p < 0.001$) of total growth with complete growth inhibition at 400 μg/ml. Reduction in molecular weight enhanced the activity at lower concentrations with significantly higher ($p < 0.001$) growth reduction at stationary phase. The reduction in molecular weight from 165 to 47 kDa was associated with a 1% increase in DD and an increase in pKa from 6.38 to 6.68; while the changes in DD and pKa can enhance the antibacterial activity, there is evidence in literature that a molecular weight around 50 kDa is less effective than higher molecular weights (Costa et al., 2012), therefore the overall effect observed for CS3H was not as significant as desired. Further modification with the addition of less-hindered amino groups was investigated as a way to enhance activity as low molecular weight polymers will be preferred and easier formulated. This was not the case with CS3H $EtNH_2$ possibly due to the reduced solubility of the polymer. CS3H Lys instead showed enhanced activity with complete inhibition of bacterial growth at 200 μg/ml. The better performance of CS3H Lys showed that pKa or molecular weight are not good predictors of activity on their own. We hypothesise that here the presence of less hindered amino groups and the possible hydrophobic interactions that the C6 chain can establish with the bacterial wall are responsible for the enhanced activity (Ardean et al., 2021). Due to the limited solubility and the failure to enhance antibacterial efficacy CS3H $EtNH_2$ was not further investigated. Chitosan polymers were tested also against the Gram-negative *P. aeruginosa*, all polymers induced complete growth inhibition starting from 100 μg/ml demonstrating that this strain is more susceptible to the action of chitosan independently from molecular weight and pKa. Cytotoxicity of the polymers was assessed against osteoblasts. CS showed high cytocompatibility with cell viability higher than 70% even at concentrations as high as 800 μg/ml. CS3H presented reduced toxicity compared to the higher molecular weight polymer, with significant reduction in cell viability observed only at 400 μg/ml (compared to 200 μg/ml for CS). Both CS and CS3H presented significant toxicity at concentrations above 1 mg/ml, this observation has not been reported in literature before as there are no reports of cytotoxicity testing of chitosan solutions on osteoblasts. More commonly scaffolds containing or composed of chitosan in the solid state are tested on osteoblasts (Koski et al., 2020). However, there is evidence of cytotoxicity against other cell lines for example a reduction of cell viability to ca. 70% has been reported for depolymerised (50 kDa) glycol chitosan tested on chondrocytes (Knight et al., 2007), while Huang et al. reported significant toxicity of chitosan solutions at concentrations above 0.7 mg/ml against A549 cells (Huang et al., 2004). CS3H Lys caused a reduction in viability of 30% at the lowest concentration tested with 65% viability at 200 μg/ml the minimum concentration that elicits complete inhibition of *S. aureus* growth. However, these results alone are

not conclusive in regards to cytotoxicity as other effects due to the lysine pendant chain could be at play. For example, lysine-decorated nanoparticles have been developed for pH specific adsorption of organic dyes so CS3H Lys might interact with MTT reducing the amount of dye absorbed and therefore metabolised by the cells giving a lower signal that is not necessarily associated with higher toxicity (Jing et al., 2018). On the other hand MTT might favour cell and mitochondria internalisation of CS3H Lys that could have an inhibitory (Zhou et al., 2019) or promoting (De Marchi et al., 2019) effect on mitochondrial metabolism. Therefore, the MTT results need to be interpreted with caution in regards to the suggested cytotoxicity of CS3H Lys and further studies using flow cytometry are required. Further studies will focus on the development of composite materials containing CS3H Lys as coatings for orthopaedic implants. This material also has potential in applications for wound healing and as component of dental hygiene products (Rahayu et al., 2022).

5. Conclusion

In summary, we have successfully synthesised and characterised two novel chitosan derivatives: CS3H $EtNH_2$ and CS3H Lys with lower molecular weight and a higher pKa value compared to the original chitosan. The original and modified chitosan polymers presented antibacterial activities against *S. aureus* and *P. aeruginosa*, with CS3H Lys having the highest effect against *S. aureus*. Although an MTT assay showed that this polymer can be potentially reducing the number of metabolically active osteoblast cells, more studies are needed to support these data as the grafted lysine chain might interfere with the MTT dye.

CRediT authorship contribution statement

Dien Puji Rahayu: Methodology, Formal analysis, Investigation, Writing – original draft, Visualization, Funding acquisition. **Arianna De Mori:** Investigation, Methodology, Writing – review & editing. **Rahmi Yusuf:** Investigation. **Roger Draheim:** Methodology, Resources, Writing – review & editing. **Aikaterini Lalatsa:** Conceptualization, Methodology, Resources, Writing – review & editing. **Marta Roldo:** Conceptualization, Methodology, Resources, Writing – original draft, Writing – review & editing, Supervision, Funding acquisition.

Declaration of competing interest

The authors declare that they have no known competing financial interests or personal relationships that could have appeared to influence the work reported in this paper.

Acknowledgements

This project was funded through the scholarship Program for Research and Innovation in Science and Technology (RISET-Pro) by the Ministry of Research, Technology and Higher Education of the Republic of Indonesia (World Bank Loan No. 8245-ID).

Appendix A. Supplementary data

Supplementary data to this article can be found online at https://doi.org/10.1016/j.carbpol.2022.119385.

References

Abd El-Hack, M. E., El-Saadony, M. T., Shafi, M. E., Zabermawi, N. M., Arif, M., Batiha, G. E., Khafaga, A. F., Abd El-Hakim, Y. M., & Al-Sagheer, A. A. (2020). Antimicrobial and antioxidant properties of chitosan and its derivatives and their applications: A review. *International Journal of Biological Macromolecules, 164*, 2726–2744. https://doi.org/10.1016/j.ijbiomac.2020.08.153

Abedian, Z., Jenabian, N., Moghadamnia, A. A., Zabihi, E., Tashakorian, H., Rajabnia, M., Sadighian, F., & Bijani, A. (2019). Antibacterial activity of high-molecular-weight and low-molecular-weight chitosan upon oral pathogens. *Journal of Conservative Dentistry, 22*(2), 169–174. https://doi.org/10.4103/JCD.JCD

Aljbour, N. D., Beg, M. D. H., & Gimbun, J. (2019). Acid hydrolysis of chitosan to oligomers using hydrochloric acid. *Chemical Engineering Technology, 42*(9), 1741–1746. https://doi.org/10.1002/ceat.201800527

Arciola, C. R., & Campoccia, D. (2018). Implant infections: Adhesion, biofilm formation and immune evasion. *Nature Reviews Microbiology, 16*(July), 397–409. https://doi.org/10.1038/s41579-018-0019-y

Ardean, C., Davidescu, C. M., Nemeş, N. S., Negrea, A., Ciopec, M., Duteanu, N., Negrea, P., Duda-Seiman, D., & Musta, V. (2021). Factors influencing the antibacterial activity of chitosan and chitosan modified by functionalization. *International Journal of Molecular Sciences, 22*(14). https://doi.org/10.3390/ijms22147449

Campoccia, D., Montanaro, L., & Arciola, C. R. (2006). The significance of infection related to orthopedic devices and issues of antibiotic resistance. *Biomaterials, 27*(11), 2331–2339. https://doi.org/10.1016/j.biomaterials.2005.11.044

Chao, D., Xin, M., Jingru, M., Khan, M. I. H., Lei, D., Avik, K., Xingye, A., Junhua, Z., Huq, T., & Yonghao, N. (2019). Chitosan as a preservative for fruits and vegetables: A review on chemistry and antimicrobial properties. *Journal of Bioresources and Bioproducts, 1*(1). https://doi.org/10.21967/jbb.v2i4.163

Cheah, W. Y., Show, P. L., Ng, I. S., Lin, G. Y., Chiu, C. Y., & Chang, Y. K. (2019). Antibacterial activity of quaternized chitosan modified nanofiber membrane. *International Journal of Biological Macromolecules, 126*, 569–577. https://doi.org/10.1016/j.ijbiomac.2018.12.193

Costa, E. M., Silva, S., Pina, C., Tavaria, F. K., & Pintado, M. M. (2012). Evaluation and insights into chitosan antimicrobial activity against anaerobic oral pathogens. *Anaerobe, 18*(3), 305–309. https://doi.org/10.1016/j.anaerobe.2012.04.009

Costa-Pinto, A. R., Lemos, A. L., Tavaria, F. K., & Pintado, M. (2021). Chitosan and hydroxyapatite based biomaterials to circumvent periprosthetic joint infections. *Materials, 14*(4). https://doi.org/10.3390/ma14040804

De Marchi, U., Galindo, A. N., Thevenet, J., Hermant, A., Bermont, F., Lassueur, S., Domingo, J. S., Kussmann, M., Dayon, L., & Wiederkehr, A. (2019). Mitochondrial lysine deacetylation promotes energy metabolism and calcium signaling in insulin-secreting cells. *FASEB Journal, 33*(4), 4660–4674. https://doi.org/10.1096/fj.201801424R

Einbu, A., & Vårum, K. M. (2007). Depolymerization and De-N-acetylation of chitin oligomers in hydrochloric acid. *Biomacromolecules, 8*, 309–314. https://doi.org/10.1021/bm0608535

Gerecht, S., Sun, G., & Shen, Y.-I. (2011). *EP2588125A4*.

Goy, R. C., de Britto, D., & Assis, O. B. G. (2009). A review of the antimicrobial activity of chitosan. *Polímeros, 19*(3), 241–247. https://doi.org/10.1590/S0104-14282009000300013

Hamill, P. G., Stevenson, A., McMullan, P. E., Williams, J. P., Lewis, A. D. R., Sudharsan, S., Stevenson, K. E., Farnsworth, K. D., Khroustalyova, G., Takemoto, J. Y., Quinn, J. P., Rapoport, A., & Hallsworth, J. E. (2020). Microbial lag phase can be indicative of, or independent from, cellular stress. *Scientific Reports, 10*(1), 1–20. https://doi.org/10.1038/s41598-020-62552-4

Hermanson, G. T. (2013). sciencedirect-topic-2-bromoethylamine.pdf. In *Bioconjugate techniques* (3rd ed., pp. 1095–1146). Academic Press, 3rd ed.

Hirai, A., Odani, H., & Nakajima, A. (1991). Determination of degree of deacetylation of chitosan by 1H NMR spectroscopy. *Polymer Bulletin, 26*(1), 87–94. https://doi.org/10.1007/BF00299352

Hu, L., Meng, X., Xing, R., Liu, S., Chen, X., Qin, Y., Yu, H., & Li, P. (2016). Design, synthesis and antimicrobial activity of 6-N-substituted chitosan derivatives. *Bioorganic and Medicinal Chemistry Letters, 26*(18), 4548–4551. https://doi.org/10.1016/j.bmcl.2015.08.047

Huang, M., Khor, E., & Lim, L.-Y. (2004). *Uptake and Cytotoxicity of Chitosan Molecules and Nanoparticles: Effects of Molecular Weight and Degree of Deacetylation*.

Jiang, M., Wang, K., Kennedy, J. F., Nie, J., Yu, Q., & Ma, G. (2010). Preparation and characterization of water-soluble chitosan derivative by Michael addition reaction. *International Journal of Biological Macromolecules, 47*(5), 696–699. https://doi.org/10.1016/j.ijbiomac.2010.09.002

Jing, S., Wang, X., & Tan, Y. (2018). Preparation of lysine-decorated polymer-brush-grafted magnetic nanocomposite for the efficient and selective adsorption of organic dye. *Applied Surface Science, 441*, 654–662. https://doi.org/10.1016/j.apsusc.2018.01.259

Kasaai, M. R., Arul, J., & Charlet, G. (2013). Fragmentation of chitosan by acids. *The Scientific World Journal, 2013*, 1–11. https://doi.org/10.1155/2013/508540

Kasaai, R. (2009). Various methods for determination of the degree of N-acetylation of chitin and chitosan: A review. *Journal of Agricultural and Food Chemistry, 57*, 1667–1676.

Knight, D. K., Shapka, S. N., & Amsden, B. G. (2007). Structure, depolymerization, and cytocompatibility evaluation of glycol chitosan. *Journal of Biomedical Materials Research - Part A, 83*(3), 787–798. https://doi.org/10.1002/jbm.a.31430

Koski, C., Vu, A. A., & Bose, S. (2020). Effects of chitosan-loaded hydroxyapatite on osteoblasts and osteosarcoma for chemopreventative applications. *Materials Science and Engineering C, 115*. https://doi.org/10.1016/j.msec.2020.111041

Kubota, N., Tatsumoto, N., Sano, T., & Toya, K. (2000). A simple preparation of half N-acetylated chitosan highly soluble in water and aqueous organic solvents. *Carbohydrate Research, 324*(4), 268–274. https://doi.org/10.1016/S0008-6215(99)00263-3

Kulawik, P., Jamróz, E., & Özogul, F. (2019). Chitosan role for shelf-life extension of seafood. *Environmental Chemistry Letters, October*. https://doi.org/10.1007/s10311-019-00935-4

Lalatsa, A., Garrett, N. L., Ferrarelli, T., Moger, J., Schätzlein, A. G., & Uchegbu, I. F. (2012). Delivery of peptides to the blood and brain after oral uptake of quaternary

ammonium palmitoyl glycol chitosan nanoparticles. *Molecular Pharmaceutics, 9*(6), 1764–1774. https://doi.org/10.1021/mp300068j

Lalatsa, A., Schätzlein, A. G., Garrett, N. L., Moger, J., Briggs, M., Godfrey, L., Iannitelli, A., Freeman, J., & Uchegbu, I. F. (2015). Chitosan amphiphile coating of peptide nanofibres reduces liver uptake and delivers the peptide to the brain on intravenous administration. *Journal of Controlled Release, 10*(197), 87–96. https://doi.org/10.1016/j.jconrel.2014.10.028

Li, J., Fu, J., Tian, X., Hua, T., Poon, T., Koo, M., & Chan, W. (2022). Characteristics of chitosan fiber and their effects towards improvement of antibacterial activity. *Carbohydrate Polymers, 280*(December 2021), Article 119031. https://doi.org/10.1016/j.carbpol.2021.119031

Li, J., Wu, Y., & Zhao, L. (2016). Antibacterial activity and mechanism of chitosan with ultra high molecular weight. *Carbohydrate Polymers, 148*, 200–205. https://doi.org/10.1016/j.carbpol.2016.04.025

Mao, S., Shuai, X., Unger, F., Simon, M., Bi, D., & Kissel, T. (2004). The depolymerization of chitosan: Effect on physicochemical and biological properties. *International Journal of Pharmaceutics, 281*, 45–54.

Mullis, A. S., Peroutka-Bigus, N., Phadke, K. S., Bellaire, B. H., & Narasimhan, B. (2021). Nanomedicines to counter microbial barriers and antimicrobial resistance. *Current Opinion in Chemical Engineering, 31*, Article 100672. https://doi.org/10.1016/j.coche.2021.100672

Oliveira, W. F., Silva, P. M. S., Silva, R. C. S., Silva, G. M. M., Machado, G., Coelho, L. C. B. B., & Correia, M. T. S. (2018). Staphylococcus aureus and Staphylococcus epidermidis infections on implants. *Journal of Hospital Infection, 98*(2), 111–117. https://doi.org/10.1016/j.jhin.2017.11.008

Panda, P. K., Yang, J. M., Chang, Y. H., & Su, W. W. (2019). Modification of different molecular weights of chitosan by p-coumaric acid: Preparation, characterization and effect of molecular weight on its water solubility and antioxidant property. *International Journal of Biological Macromolecules, 136*, 661–667. https://doi.org/10.1016/j.ijbiomac.2019.06.082

Rahayu, D. P., De Mori, A., Draheim, R., Lalatsa, K., & Roldo, M. (2022). Harnessing the properties of fluoridated chitosan polymers against the formation of oral biofilms. *Pharmaceutics, 14*(3), 488–502. https://doi.org/10.3390/pharmaceutics14030488

Rahmani, S., Mohammadi, Z., Amini, M., Isaei, E., Taheritarigh, S., Rafiee Tehrani, N., & Rafiee Tehrani, M. (2016a). Methylated 4-N, N dimethyl aminobenzyl N, O carboxymethyl chitosan as a new chitosan derivative: Synthesis, characterization, cytotoxicity and antibacterial activity. *Carbohydrate Polymers, 149*, 131–139. https://doi.org/10.1016/j.carbpol.2016.04.116

Roldo, M., & Fatouros, G. D. (2011). Chitosan derivative based hydrogels as drug delivery platforms. In M. Zilberman (Ed.), *Biomaterials and Nanostructures for Active Implants*. Springer.

Romanelli, S. M., Hartnett, J. W., & Banerjee, I. A. (2015). Effects of amide side chains on nanoassembly formation and gelation of fmoc-valine conjugates. *Powder Technology, 271*, 76–87. https://doi.org/10.1016/j.powtec.2014.10.028

Sahariah, P., Cibor, D., Zielińska, D., Hjálmarsdóttir, M., Stawski, D., & Másson, M. (2019). The effect of molecular weight on the antibacterial activity of N, N, N-trimethyl chitosan (TMC). *International Journal of Molecular Sciences, 20*(7). https://doi.org/10.3390/ijms20071743

Siew, A., Le, H., Thiovolet, M., Gellert, P., Schatzlein, A., & Uchegbu, I. (2012). Enhanced oral absorption of hydrophobic and hydrophilic drugs using quaternary ammonium palmitoyl glycol chitosan nanoparticles. *Molecular Pharmaceutics, 9*(1), 14–28. https://doi.org/10.1021/mp200469a, 1.

Sivashankari, P. R., & Prabaharan, M. (2016). Deacetylation modification techniques of chitin and chitosan. In chitosan based. *Biomaterials, 1*, Elsevier. https://doi.org/10.1016/B978-0-08-100230-8.00005-4

Tan, H., Ma, R., Lin, C., Liu, Z., & Tang, T. (2013). Quaternized chitosan as an antimicrobial agent: Antimicrobial activity, mechanism of action and biomedical applications in orthopedics. *International Journal of Molecular Sciences, 14*(1), 1854–1869. https://doi.org/10.3390/ijms14011854

Vårum, K. M., Myhr, M. M., Hjerde, R. J. N., & Smidsrød, O. (1997). In vitro degradation rates of partially N-acetylated chitosans in human serum. *Carbohydrate Research, 299*(1–2), 99–101. https://doi.org/10.1016/S0008-6215(96)00332-1

Yuan, Y., Chesnutt, B. M., Haggard, W. O., & Bumgardner, J. D. (2011). Deacetylation of chitosan: Material characterization and in vitro evaluation via albumin adsorption and pre-osteoblastic cell cultures. *Materials, 4*, 1399–1416. https://doi.org/10.3390/ma4081399

Zhang, Q., Wang, C., Qiao, L., Yan, H., & Liu, K. (2009). Superparamagnetic iron oxide nanoparticles coated with a folate-conjugated polymer. *Journal of Materials Chemistry, 19*(44), 8393–8402. https://doi.org/10.1039/b910439a

Zhou, J., Wang, X., Wang, M., Chang, Y., Zhang, F., Ban, Z., Tang, R., Gan, Q., Wu, S., Guo, Y., Zhang, Q., Wang, F., Zhao, L., Jing, Y., Qian, W., Wang, G., Guo, W., & Yang, C. (2019). The lysine catabolite saccharopine impairs development by disrupting mitochondrial homeostasis. *Journal of Cell Biology, 218*(2), 580–597. https://doi.org/10.1083/jcb.201807204